The EMBO Journal (2004), 1–7 | © 2004 European Molecular Biology Organization | All Rights Reserved 0261-4189/04
www.embojournal.org

THE EMBO JOURNAL

Variable LH2 stoichiometry and core clustering in native membranes of *Rhodospirillum photometricum*

Simon Scheuring[1,*], Jean-Louis Rigaud[1] and James N Sturgis[2]

[1]Institut Curie, UMR-CNRS 168 and LRC-CEA 34V, Paris, France and [2]UPR-9027 LISM, IBSM, CNRS, Marseille, France

The individual components of the photosynthetic unit (PSU), the light-harvesting complexes (LH2 and LH1) and the reaction center (RC), are structurally and functionally known in great detail. An important current challenge is the study of their assembly within native membranes. Here, we present AFM topographs at 12 Å resolution of native membranes containing all constituents of the PSU from *Rhodospirillum photometricum*. Besides the major technical advance represented by the acquisition of such highly resolved data of a complex membrane, the images give new insights into the organization of this energy generating apparatus in *Rsp. photometricum*: (i) there is a variable stoichiometry of LH2, (ii) the RC is completely encircled by a closed LH1 assembly, (iii) the LH1 assembly around the RC forms an ellipse, (iv) the PSU proteins cluster together segregating out of protein free lipid bilayers, (v) core complexes cluster although enough LH2 are present to prevent core–core contacts, and (vi) there is no cytochrome bc1 complex visible in close proximity to the RCs. The functional significance of all these findings is discussed.

The EMBO Journal advance online publication, 30 September 2004; doi:10.1038/sj.emboj.7600429
Subject Categories: structural biology; membranes & transport
Keywords: AFM; bacterial photosynthesis; light harvesting; membrane protein organization; PSU

Introduction

Photosynthetic organisms fuel their metabolism with light energy and have developed for this purpose a highly efficient apparatus consisting of multiple membrane proteins. The bacterial photosynthetic unit (PSU) is made up of three different protein complexes—LH2s, LH1s, and reaction centers (RCs). Of the RC, high-resolution structures are available from *Blastochloris (Bcl.) viridis* and *Rhodobacter (Rb.) sphaeroides* (Deisenhofer *et al*, 1984, 1985, 1995; Allen *et al*, 1987; Deisenhofer and Michel, 1989). Two high-resolution structures of LH2 from *Rhodopseudomonas (Rps.) acidophila* revealing a nonameric ring assembly (McDermott *et al*, 1995; Papiz *et al*, 2003), and of *Phaeospirillum (Phsp.) molischianum* forming an octameric assembly (Koepke *et al*, 1996) are equally available. So far, no atomic level structure of the core complex, formed from LH1 and the RC, is available. However, data of three different core complexes at resolution sufficient to delineate the LH1 assembly around the RC are available: a cryo-EM projection at 8.5 Å resolution of *Rhodospirillum (Rsp.) rubrum* (Jamieson *et al*, 2002), an AFM topography at 10 Å resolution of *Blc. viridis* (Scheuring *et al*, 2003b), and a 3D structure at 4.8 Å resolution (the highest resolution) of the core complex of *Rps. palustris* revealing the backbone of the peptides (Roszak *et al*, 2003). Furthermore, low-resolution cryo and negative stain EM studies reported a 30 Å gap in the LH1 assembly of the dimeric PufX containing core complex of *Rb. sphaeroides* (Jungas *et al*, 1999; Scheuring *et al*, 2004a; Siebert *et al*, 2004). Taking together, the core complex was described to consist of an RC surrounded by an ellipse of 16 LH1 α/β heterodimers (*Rsp. rubrum*, *Blc. viridis*), 15 LH1 α/β heterodimers plus one PufX-like peptide (*Rps. palustris*), or 12 LH1 α/β heterodimers plus one PufX plus a gap (*Rb. sphaeroides*). It thus appears that core complexes have different architectures in different species, and it is expected that these structural differences have significant functional effects.

All this structural information on the individual components, in addition to functional measurements, has formed the basis of numerous models of the PSU (Papiz *et al*, 1996; Hu *et al*, 1998, 2002; Sundström *et al*, 1999; Frese *et al*, 2000). All components of the PSU cooperate in light energy capturing and channeling to the RC. However, to date, no detailed data of the architecture and interplay between these proteins of the PSU had been presented. Initial AFM images at low and medium resolution recently allowed us to describe the organization of the complex assembly in native membranes (Scheuring *et al*, 2004b). Now, we have acquired topographs at 12 Å resolution of the native photosynthetic membrane of *Rhodospirillum photometricum*. These new images allow us to report on the structural heterogeneity in the LH2, which results in a variable stoichiometry within the membranes, and to get more detailed insight into the interactions of the individual components in the PSU.

Results and discussion

High-resolution imaging

High-resolution AFM topographs of the native photosynthetic membranes of *Rsp. photometricum* could be acquired (Figure 1). In spite of the slight nonflatness of the adsorption of the native membranes, large patches could be imaged at submolecular resolution (Figure 1A). A series of images at high magnification (Figure 1B) allowed the calculation of

*Corresponding author. Institut Curie, UMR-CNRS 168 and LRC-CEA 34V, 11 rue Pierre et Marie Curie, 75231 Paris Cedex 05, France.
Tel.: +33 1 4234 6775; Fax: +33 1 4051 0636;
E-mail: simon.scheuring@curie.fr

Received: 22 July 2004; accepted: 7 September 2004

averages (Figure 1C) of the different components of the PSU using reference free single-particle alignment procedures (see Materials and methods). Signal-to-noise analysis (Unser *et al*, 1987, 1989) indicated that we have reliable information to 15 Å resolution in the core-complex average, and to 12 Å resolution in the LH2 complex average.

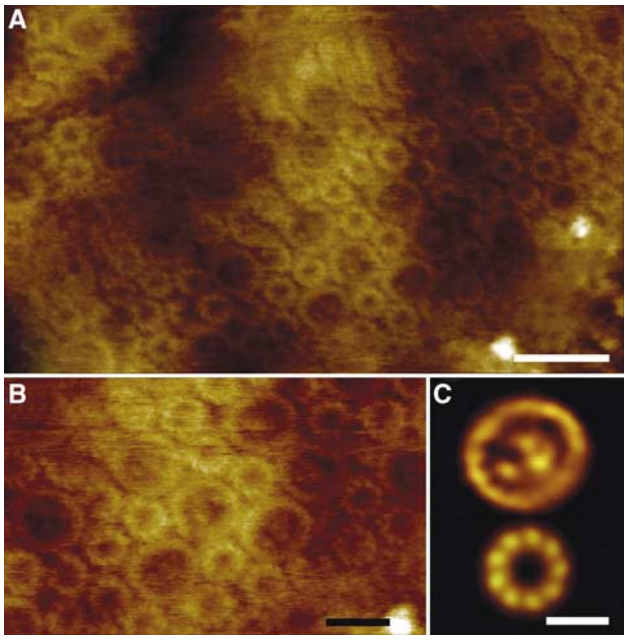

Figure 1 High-resolution AFM of native photosynthetic membranes of *Rsp. photometricum*. (**A**) Large native membrane patch (128 nm) at submolecular resolution (scale bar: 20 nm; full color scale: 6 nm). (**B**) Close-up view of an assembly of multiple core complexes and LH2s. Topography substructure can be seen on the individual LH2 and RC molecules (scale bar: 10 nm; full color scale: 6 nm). (**C**) Averages of the core complexes (top, 15 Å resolution) and the LH2 (bottom, 12 Å resolution) calculated from two hand-picked families of 235 and 1301 particles, respectively (scale bar: 20 nm; full color scale: 2 nm).

The light-harvesting complexes

The majority of the LH2 were aligned and averaged to give a ring shaped assembly with nine-fold symmetry (Figure 1C, bottom). However, on closer examination of the raw data images, it is obvious that LH complexes of various sizes are present within the native membranes (Figure 2A–D), providing a first indication of the heterogeneity of the LH2 complex stoichiometry. Indeed ~70% of the complexes had a top ring diameter of 46 Å < *d* < 54 Å, in agreement with that measured for nonameric LH2 of *Rubrivivax (Rvi.) gelatinosus*, *Rb. sphaeroides*, and *Rsp. acidophila* (Scheuring *et al*, 2001, 2003a; Gonçalves *et al*, 2004). In contrast, the remaining

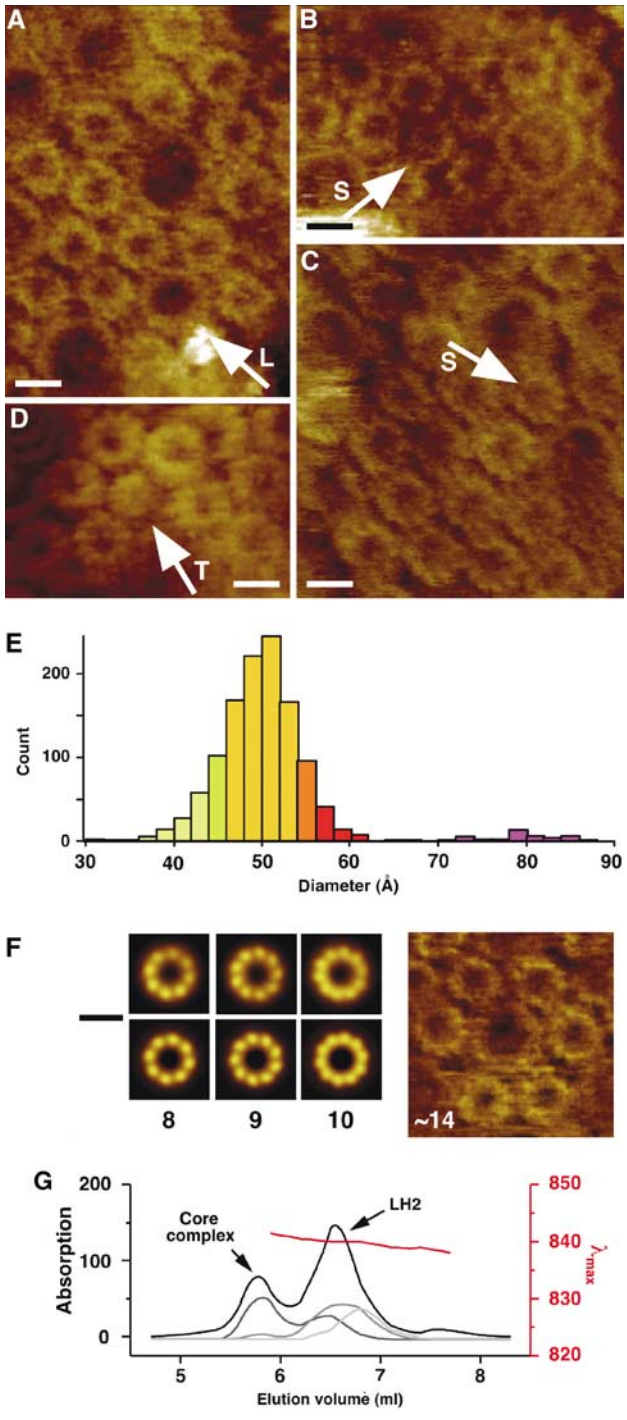

Figure 2 Diversity of LH complexes. (**A**) A large ~80 Å diameter (arrow L) light-harvesting complex, (**B, C**) small ~40 Å diameter (arrow S) light-harvesting complexes, and (**D**) a tiny (arrow T) particle in assembly with LH2s and core complexes (all scale bars: 5 nm; full color scale: 4 nm). (**E**) Graph reporting the abundance of different-sized LH complexes. The analysis of the diameter of the complexes represents a Gaussian distribution peaking at 50 Å. A small fraction of LH complexes with diameters up to ~85 Å are detected. (**F**) Averages of the LH components calculated after classification of their rotational power spectra (as described in Materials and methods). From the most abundant complexes with diameters around 50 Å, three classes with 8-, 9-, and 10-fold symmetry could be calculated. A representative complex with a diameter of ~80 Å is shown surrounded by six 'normal' LH2s. Judged from its size, we estimate this complex to consist of ~14 LH subunits. These complexes were rare and strongly variable in size inhibiting the calculation of an average (scale bars: 5 nm; full color scale: 2 nm). (**G**) Gel exclusion chromatography analysis of the complex size heterogeneity of LH2. In initial elution (black line), the fraction size was 100 µl. Re-chromatography of three fractions eluting at 6.0 ml (dark gray line), 6.5 ml (medium gray line), and 7.0 ml (light gray line). The red line displays the near-infrared absorption maximum of the elution fractions (right red *Y*-axis). The larger complexes absorb at 841 nm and the latest eluting smallest complexes at 838.5 nm.

~30% of the complexes had either significantly smaller ($d<46$ Å) or larger ($d>54$ Å) diameters (Figure 2E). Correspondingly, separation of the particles using neuronal network classification of their rotational power spectrum revealed fractions of particles incompatible with nine-fold symmetry, giving a signal for 8- or 10-fold symmetry (Figure 2F).

In this context, it is interesting to recall that the crystallographic LH2 structure of *Rps. acidophila* revealed a nonamer, while the structure of *Phsp. molischianum* was octameric (McDermott *et al*, 1995; Koepke *et al*, 1996). Furthermore, EM and AFM studies revealed nonameric organizations for LH2s from *Rhodovulum (Rhv.) sulfidophilum*, *Rb. sphaeroides*, and *Rvi. gelatinosus* (Montoya *et al*, 1995; Walz *et al*, 1998; Ranck *et al*, 2001; Scheuring *et al*, 2001, 2003a). A low light LH2 from *Rps. palustris* was compatible with eight-fold symmetry (Hartigan *et al*, 2002). Thus, there are already reports of interspecies heterogeneity with octameric and nonameric LH2.

Currently, the only structural heterogeneity within a species that has been described is based on a medium-resolution AFM analysis of solubilized, purified, and reconstituted LH1 lacking the RC (Bahatyrova *et al*, 2004). Here, we show for the first time heterogeneity in the size of LH2 in one species. Since the images are acquired on native membranes of *Rsp. photometricum*, the proteins have never been in contact with detergent or any other denaturant, reinforcing that the heterogeneity found represents an inherent feature of native LH2 assembly. At a molecular level, such variability in the ring size requires small changes in the interaction angle between adjacent subunits, 45, 40, and 36° for 8-, 9-, and 10-subunit complexes, respectively. This variability requires some structural flexibility. In the LH2 structures, interactions supporting the oligomerization are governed through van der Waals interactions and a set of hydrogen bonds (Koepke *et al*, 1996). Hydrogen bonds allow variability in length and angle superior to the angular differences required for different oligomeric states, representing a possible explanation (Creighton, 1993).

To further investigate this heterogeneity, solubilized membranes were analyzed by size exclusion chromatography. After solubilization by dodecyl-maltoside, besides a peak containing the core complexes, the LH2 eluted from the gel filtration as a relatively broad peak (Figure 2G, black line). Re-chromatography of individual fractions confirmed the size heterogeneity of the LH2 found in high-resolution AFM topographs. Fractions from the beginning of the peak reproducibly eluted earlier than fractions from the end of the peak on re-chromatography (Figure 2G, gray lines). Furthermore, this hydrodynamic heterogeneity is accompanied by a spectral heterogeneity. The LH2 absorption peak in membranes of *Rsp. photometricum* changes slightly with culture conditions, varying between 839 and 846 nm. This variability is attributed to heterogeneity in the polypeptides expressed from a multi *puc*-operon family as previously observed in *Phsp. molischianum* (Germeroth *et al*, 1996) or *Rps. palustris* (Tadros and Waterkamp, 1989). The LH2 in the *Rsp. photometricum* membranes analyzed in these experiments had a near-infrared absorption maximum at 841 nm in the membrane. However, the absorption maxima for the different fractions of solubilized LH2 after size exclusion chromatography showed that the maximum varied from 841.0 nm at the beginning to 838.5 nm at the end of the peak (Figure 2G, red line). Thus hydrodynamically larger LH2s appear to have more red absorption than hydrodynamically smaller LH2.

The size heterogeneity found around the nine-fold modal value could be a general feature in photosynthetic bacteria. This variability could represent a strategy for generating a broader absorption and thus maximizing light absorption, or a strategy for optimizing packing in a heterogeneous membrane.

On the other hand, the heterogeneity might be a cause of the difficulties faced with the growth of 3D crystals for X-ray analysis of these complexes. It will be interesting to know what percentage of crystals analyzed to yield the atomic structures known diffracted to high resolution (McDermott *et al*, 1995; Koepke *et al*, 1996). Although usually for 3D crystallization stringent size exclusion chromatographies are used, one could speculate that 3D crystals, which do not diffract to high resolution, are formed by mixtures of oligomeric states of the LH2 complexes.

The AFM with its high signal-to-noise ratio allows single molecules to be detected and analyzed. Thus, in addition to the statistically important octameric, nonameric, and decameric rings, several rarer structures are observed. A minor fraction forms large rings with a diameter of ~80 Å (Figure 2E). The size heterogeneity and the small number of particles in this class made the calculation of an average impossible. However, as judged from the diameter of these individual complexes, they consist of up to 14 subunits (Figure 2F). They might be explained as particularly large LH2 assemblies or particularly small LH1 assemblies, where no RC subunits were integrated during biosynthesis.

A particularly defective complex is shown in Figure 3B. A moon-shaped LH2 probably consisting of ~4 LH2 subunits (arrow M) can be seen. We cannot conclusively decide whether this finding is due to destruction induced by increased loading forces applied to the tip, or if it is due to imperfections during biosynthesis of the complex.

The core complex

In contrast to the heterogeneity found for LH2 complexes, the LH1 assemblies of the core complexes appear uniform in size, when the RC proteins are present. The LH1 assembly of the core complex forms a closed ellipse with long and short axes of 95 and 85 Å, respectively; within this, an asymmetric RC topography is seen (Figure 1C, top). The finding of an LH1 ellipse with long and short axes difference of 10% following the long RC axis is entirely in line with the EM data of 2D crystals of purified core complexes of the closely related *Rsp. rubrum* (Jamieson *et al*, 2002), and with the AFM topographs of core complexes in native membranes of *Blc. viridis* (Scheuring *et al*, 2003b) housing 16 LH1 subunits.

Again, the power of the AFM to visualize individual molecules at high resolution allows obtaining a deeper insight into the core complex structure. Among the complexes seen in the high-resolution images, sufficient to resolve single LH subunits consisting of only two transmembrane helices, individual core complexes are visible, which deviate from the general topography. First, an individual core complex is shown in Figure 3A, where the RC moiety is capped. Section profile analysis of this complex compared to a neighboring 'normal' complex shows significant additional topography (Figure 3B). This cap is interpreted as cytochrome c2 docked

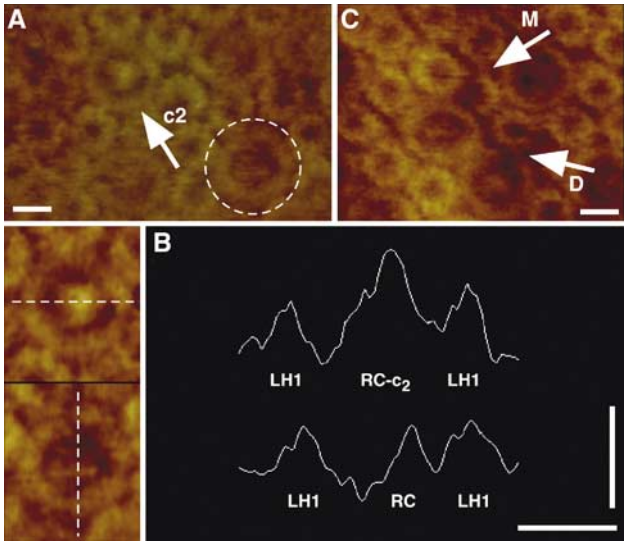

Figure 3 Observation of particular complex assemblies. (**A**) Core in which the RC is capped by additional topography interpreted as a cytochrome c2 (arrow c2) neighbored by three 'normal' cores (one of them encircled). (**B**) Section analysis of the c2 capped (top) and 'normal' (bottom) core complexes shown in (A). Right panel: Section analysis profiles along the dashed white lines in the left panel. While the RC surface of the 'normal' core complex reveals similar height as the LH1 units around, the c2 capped RC protrudes significantly stronger (horizontal scale bar: 5 nm; vertical scale bar: 1 nm). (**C**) A moon-shaped assembly of probably four LH2 subunits (arrow M) and a core in which the LH1 assembly reveals an ~20 Å gap (arrow D). While the cytochrome c2 capped core represents an intermediate state in the photosynthetic cycle, the complexes depicted in the right panel represent most certainly defective molecules (scale bars: 5 nm; full color scale: 4 nm).

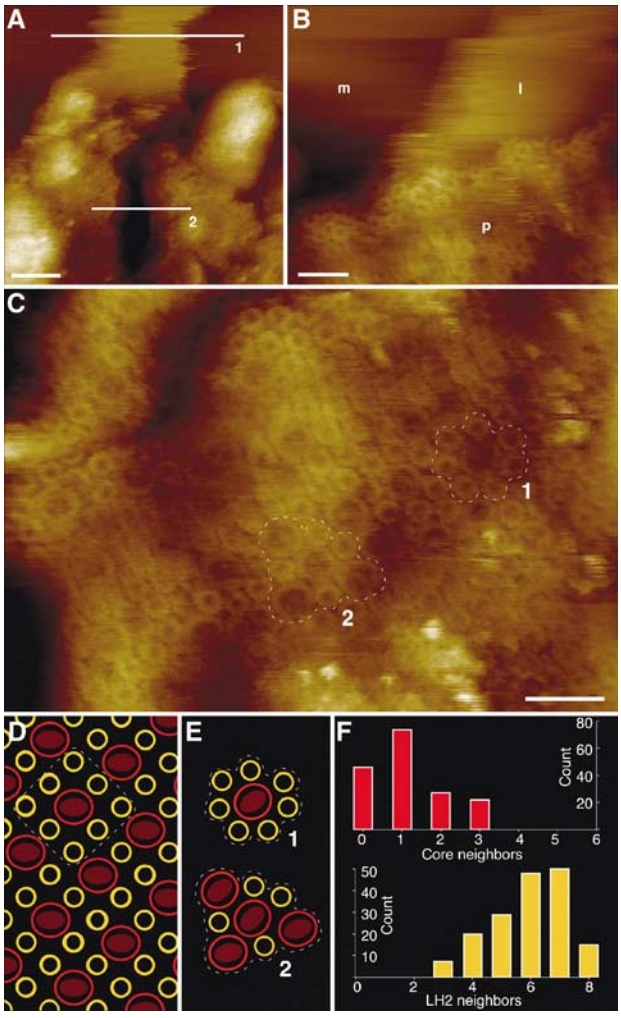

Figure 4 Arrangement of the PSU. (**A**) Overview topograph of a native membrane patch constituted of densely packed and pure lipid membrane parts. Section analysis along the two white lines (1 and 2) resulted in thickness measures of ~4 nm (line 1) and ~8 nm (line 2), respectively (scale bars: 50 nm; full color scale: 15 nm). (**B**) Boarder delineating the area containing the PSU proteins (p) from protein-free lipid bilayer (l). The smooth area in the top left is the mica AFM support (m) (scale bars: 20 nm; full color scale: 12 nm) (**C**) Medium-resolution topograph allowing the molecular arrangement of the proteins of the PSU to be studied (scale bars: 20 nm; full color scale: 10 nm). (**D**) Model membrane packing based on a PSU constituted of eight LH2s around one core (dashed line; Papiz *et al*, 1996). In such a system, each core has eight LH2 neighbors, zero contacts with other cores, while the average ratio of LH2–core complexes is 4. (**E**) Two examples (depicted in (C) by dashed contour line) of core–neighbor assemblies: (1) core in contact with seven LH2s and zero cores and (2) core in contact with four LH2s and three cores. (**F**) Graphs displaying numbers of neighboring LH2s and neighboring cores to a core. Top panel: Number of neighboring cores—'only' 27% of the cores have zero direct contact with another core, 44% have one core contact, and the remaining 29% make two or maximally three contacts with neighboring cores (see example 2 in C and E). Bottom panel: Number of neighboring LH2s—the assembly of eight LH2s surrounding a core is rarely (9%) found; in these cases, at least one of the LH2s does not make physical contact with the core. Most cores are connected with seven LH2s (30%). We never found a core with less than three direct LH2 neighbors. The average ratio of LH2/core in the membranes analyzed is ~5.

to the RC (Figure 3A, arrow c2), representing an important transient state in the photosynthetic cycle. We believe that during scanning in buffer solution the c2 diffuse away into the bulk, hence no significant fraction of the cores can be imaged capped with c2, inhibiting topography averaging. Further experiments with an excess of exogenous c2 will provide deeper insight into the LH1–RC–cyt c2 complex assembly. Second, a core complex with an interrupted LH1 assembly, an ~20 Å gap corresponding to one or two LH1 subunits, is seen (Figure 3C, arrow D). We cannot conclusively decide whether this finding (Figure 3C) is due to destruction induced by the scanning mechanism, or if it is due to imperfections during biosynthesis of the complexes. Whatever, only very few such defects can be detected, hence they do not represent significant assemblies in *Rsp. photometricum*. Moreover, the fact that the resolution and the AFM sensibility are sufficient to detect a 20 Å gap in the LH1 assembly strengthens our view of the native *Rsp. photometricum* LH1 to be a closed ellipsis around the RC.

Architecture of the photosynthetic unit

Imaging overview topographs and large membrane patches at submolecular resolution (Figure 4) allow us to analyze the assembly of PSU complexes in the membranes of *Rsp. photometricum* grown under low light conditions. Within the membrane, smooth and corrugated patches are observed (Figure 4A). Section analysis detects ~4 nm thickness for the smooth parts and ~8 nm for the corrugated parts (data not shown). We conclude that the membrane parts containing the PSU proteins are connected to protein-free lipid bilayers. A close-up view at a boarder between an area densely packed with the PSU proteins and a protein-free

lipid bilayer is shown in Figure 4B. This is an important observation, which demonstrates that all membrane proteins of the photosynthetic apparatus have a tendency to cluster together and that the generated structure is due to specific protein–protein interactions and not exclusively to the high protein concentration and packing difficulties. At higher magnification (Figure 4C), we can analyze the complex mixture of the LH2, LH1, and the RC complexes. In total, we find an LH2/core ratio of ~5 in these membranes (171/35 in the image shown in Figure 4C, where no LH2-only region is situated; a total of 1301/235 from unbiased particle picking on all images analyzed). It is immediately apparent that there is no fixed PSU structure. Indeed, we find cores completely surrounded by LH2 (Figure 4C, outline 1), and cores that make multiple core–core contacts (Figure 4C, outline 2). Indeed, only 27% of all cores make zero contact with other cores, while 73% of the cores make one, two, or maximally three core–core contacts. Correspondingly, 61% of the cores contact six or less LH2. We find a significant fraction (30%) of the cores in contact with seven LH2s, which appears to be the maximum of direct neighbors (Figure 4C and E, number 1), and not eight LH2s as modeled (Papiz *et al*, 1996; Hu *et al*, 1998, 2002). In the cases where eight LH2s are found in close proximity to a core, at least one of them does not make physical contact with the core complex.

It is possible to imagine an LH2–LH1–RC organization as shown in Figure 4D. In such a model, which is possible with an LH2:core ratio as low as 4, each core has eight LH2 neighbors, as modeled (Papiz *et al*, 1996; Hu *et al*, 1998, 2002), but zero core–core contacts. In such an arrangement, each core has a maximum absorption cross-section. Although our membranes contain in average ~5 LH2s per core, we find cores making multiple contacts, in spite of finding separated cores (Figure 4E, number 2). Theoretically, the molecules could arrange in a manner avoiding any core–core contacts (Figure 4D). This is not the case: 73% of the cores make at least one core–core contact; 29% make two contacts or more. This means, in a membrane where protein-free bilayer could be occupied (Figure 4A), that the core–core clustering must have a functional significance.

In situations when light is not limiting, it becomes probable that an exciton will arrive on a core complex, in which the RC is unavailable for photochemistry. Under these conditions, it is desirable that the exciton can visit other RCs to find one that is available for photochemistry. The transfer of the exciton from an LH1 to an LH2 is an energetically uphill process and thus requires thermal activation. In many bacterial species, the absorption maxima of LH1 and LH2 are about 875 and 850 nm, respectively, and the resulting energy difference dE is 1.6 kT at room temperature. In *Rsp. photometricum*, with its particular absorptions of LH1 (883 nm) and of LH2 (841 nm), the calculated energy difference is larger (2.6 kT); thus, the thermally activated back transfer of energy from core complexes to LH2 is much less frequent under physiological conditions. Thus the observed arrangement with multiple core–core contacts is particularly important for the function of this photosynthetic apparatus in realistic conditions. In the presence of the core–core contacts, the exciton can move along core–core connections until it finds a free RC. Interestingly, in the closely related species *Rsp. rubrum*, the presence of core dimers was proposed based on electron transfer measurements (Joliot *et al*, 1990). This global measurement on intact cells indicating coupling of cores might be explained by the core–core contacts presented in this work, where indeed most of the cores make one core–core contact.

An interesting 'negative' result is the complete absence of the cytochrome bc1 complex in the membranes imaged. While in medium-resolution topographs we previously attributed intermediate-sized membrane spaces to possible bc1 complex positions (Scheuring *et al*, 2004b), we see now, at higher resolution, that these areas were probably occupied by poorly resolved light-harvesting complexes of heterogeneous size larger than normal LH2s and smaller than core complexes (see Figure 2A). Here, we have imaged large membrane areas at high resolution (Figures 1A and 4C), which are obviously devoid of cytochrome bc1 complexes, but reveal a complex mixture of LH2, LH1, and RC. The structures of the homologous cytochrome bc1 complex from mitochondria (Xia *et al*, 1997), and of the cytochrome b6f complex from cyanobacteria and algae have been solved (Kurisu *et al*, 2003; Stroebel *et al*, 2003), all showing a dimeric arrangement with an overall size of ~5 nm × ~10 nm perpendicular to the membrane plane. Hence, if the bc1 complex would be in the membrane patches imaged, it should be easily recognizable. It seems unrealistic to presume that all the cytochrome bc1 complexes have selectively segregated away from their initial native positions, while all the RCs, LH1s, and LH2s have remained in a complex mixture. Furthermore, the arrangement of the proteins within membranes did not significantly change during the acquisition of the high-resolution topographs (about 100 min). We conclude that in these membranes very little lateral diffusional rearrangement of proteins takes place, and that we are essentially looking at native membranes isolated by two passages through a French press and a subsequent sucrose gradient centrifugation. Nevertheless, the cytochrome bc1 complex is present in the membrane preparations: its polypeptides can be found in SDS–PAGE analysis (Scheuring *et al*, 2004b), and the activity of the complex can be measured and is abolished by inhibitors of the cytochrome bc1 complex such as myxothiazole or stigmatellin (Sup.1). We suggest that in cells the cytochrome bc1 complex is located close to the cytoplasmic membrane, or on the edges of the intracytoplasmic invaginations, and that the flat surfaces of the intracytoplasmic invaginations, which we have imaged, contain the PSU proteins at high density and very little, if any, cytochrome bc1. It is possible that the PSU-dense intracytoplasmic membranes adsorb preferentially to the AFM support. However, all possible explanations implicate a location of the bc1 complex far from many of the RCs.

General conclusions

The AFM has been shown to be a powerful tool to analyze membrane proteins in reconstituted 2D lattices at submolecular resolution (Schabert *et al*, 1995). It has been suggested that it might become possible to study native membranes, in which different protein subunits interact with one another to form the functional machinery (Engel and Müller, 2000). Here, we gained topographs at 12 Å resolution of the entire PSU, consisting of the LH2, LH1, and RC proteins and a set of pigment molecules, within a native membrane. These images allow completing the picture of the organization of the antenna complexes and the RCs, giving new insights into the energy transfer from light harvesting to charge separation.

We show that the photosynthetic proteins cluster within the lipid bilayer (Figure 4A and B). We found membranes in which pure lipids and PSU-dense domains coexist (Figure 4B). Although the proteins have additional membrane space to dilute into, they cluster together. This seems reasonable and not very surprising from a functional point of view, as each light-harvesting component that segregates away from the system is nonfunctional, that is, its excitation energy after photon trapping will be lost, since it cannot pass its energy to a neighboring complex and eventually to the RC. However, the logical consequence is that the membranes containing the PSU are densely packed. Indeed, the distances between LH proteins are identical to those found in 2D crystals (Scheuring *et al*, 2001), meaning that the proteins are in physical contact with each other. Furthermore, the observed segregation depends on specific and probably relatively strong protein–protein interactions that will also reduce the dynamics of the structure. Such segregation is also entirely consistent with the observed dependence of membrane form on the composition of the PSU (Sturgis and Niederman, 1996), and indeed provides indirect support for the proposed role of the light-harvesting apparatus in controlling membrane shape (Sturgis and Niederman, 1990).

Such a close packing raises a problem to all processes, which need free diffusion within the membrane, such as the quinone/quinol (Q/QH_2) transfer between the RC and the bc1 complex. The migration of Q/QH_2 was strongly debated in light of the LH1 architecture around the RC, whether the LH1 assembly is closed or open. Of course, this is still an interesting point, but regarding a membrane in which the protein components are kept in physical protein–protein contact over several hundreds of square nanometers, the problem of Q/QH_2 passage becomes a more general problem since no bc1 is found in close proximity to the RCs. How is it possible to have, on the one hand, protein–protein contacts demanded by the functionality of the PSU within a membrane, and still allow efficient Q/QH_2 diffusion within this membrane? The transfer of redox energy between the RC and cytochrome bc1 is thus difficult to understand in light of the PSU structure: it is unclear how quinones can escape from the RC, cross the LH1 fence, and then diffuse through a densely packed membrane (in which LH2s are in physical contact), to find a relatively distant cytochrome bc1. Might there exist specific channels for diffusion, or chains of quinones to facilitate this process? First indications about large quinone pools come from exogenous cytochrome c2 oxidation measurements indicating more than 10 quinones associated to each RC (Francia *et al*, 2004).

Another important observation is the absence of cytochrome bc1 complex in the native membranes of *Rsp. photometricum*. This is after *Bcl. viridis* (Scheuring *et al*, 2003b), the second native membrane, of which we can obtain high-resolution topographs, and in both no cytochrome bc1 can be detected in close contact with the proteins of the PSU. It thus seems necessary to reconsider our preconceptions about the detailed structure of the photosynthetic membrane. The apparent problems for electron transfer from the RC to a distant cytochrome bc1 complex have now to be resolved.

Materials and methods

Bacterial culture and membrane preparation

Rsp. photometricum (DSM 121) was grown photoheterotrophically on DSM media 27 at low light intensity ($20\ W/m^2$) and harvested in late log phase. Cells were harvested and washed two times with 1 mM Tris–HCl, pH 7.0, before being broken by two passages through a French pressure cell. Lysates were loaded directly onto 5–60% sucrose gradients and centrifuged for 1.5 h. The membranes corresponding to the major pigmented band sedimented to about 40% sucrose and contained the different proteins of the photosynthetic apparatus. The membranes were washed with 1 mM Tris–HCl, pH 8, in a centrifugal concentrator and kept at 4°C for AFM analysis.

Gel exclusion chromatography

Isolated membranes were solubilized for 8 h in 1% dodecyl-maltoside. After solubilization, any nonsolubilized material was removed by centrifugation at 12 000 *g* for 20 min and the sample loaded onto a superose 6 10/300 FPLC column (Amersham Biosciences) pre-equilibrated with 20 mM Tris–HCl (pH 8) and 0.1% dodecyl-maltoside. The column was eluted with the same buffer and fractions of 100 µl were collected and analyzed for protein content and absorption.

Atomic force microscopy

Mica prepared as described (Schabert and Engel, 1994) was freshly cleaved and used as the support. The mica was immediately covered by 40 µl of adsorption buffer containing 10 mM Tris–HCl, pH 7.3, 150 mM KCl, and 20 mM $MgCl_2$. Subsequently, 2 µl of membrane solution was injected into the adsorption buffer drop on the mica surface. After 1 h, the sample was rinsed with 10 volumes of recording buffer containing 10 mM Tris–HCl (pH 7.3) and 150 mM KCl. Imaging was performed with a commercial Nanoscope-E contact-mode AFM (from Digital Instruments, Santa Barbara, CA) equipped with a low-noise laser, and a 160 µm scanner (J-scanner) using oxide-sharpened Si_3N_4 cantilevers with a length of 100 µm ($k = 0.09$ N/m; Olympus Ltd, Tokyo, Japan). For imaging, minimal loading forces of $\sim$100 pN were applied, at scan frequencies of $\sim$4 Hz ($\sim$1200 nm/s) using optimized feedback parameters. The piezo precision was determined on protein 2D crystals, at scan ranges between 100 and 300 nm, and errors in *x*- and *y*-dimensions smaller than 2% were found.

Image analysis

Averages of LH2 and the core complexes were calculated from 48 trace and retrace images acquired at different magnifications (a total of 1301 LH2 and 235 core complexes were extracted) using the Xmipp single-particle analysis program package (Marabini *et al*, 1996). Each particle was rotationally symmetrized (360-fold), and centered against the resulting 'ring image'. These centered particles were the starting point for all subsequent analysis. For the analysis of the LH diameters, each individual centered particle was again rotationally symmetrized (360-fold) and its top ring diameter was measured. For averaging, the rotational power spectrum of each particle was calculated. The rotational power spectra were classified using a neuronal network. The resolution of the averages was determined using the signal-to-noise criterion (Unser *et al*, 1987, 1989); the average images were filtered at the computed resolution.

Supplementary data

Supplementary data are available at *The EMBO Journal* Online.

Acknowledgements

We thank Drs Sergio Marco and Thomas Boudier for help with the single-particle analysis, Valerie Prima for help with membrane preparations, and Daniel Levy for fruitful discussions. This study was supported by the Institut Curie, the CEA, the CNRS, the INSERM, and an 'ACI Nanosciences 2004' grant (NR206).

References

Allen JP, Feher G, Yeates TO, Komiya H, Rees DC (1987) Structure of the reaction center from *Rhodobacter sphaeroides* R-26: the protein subunits. *Proc Natl Acad Sci USA* **84:** 6162–6166

Bahatyrova S, Frese RN, Van Der Werf KO, Otto C, Hunter CN, Olsen JD (2004) Flexibility and size heterogeneity of the LH1 light harvesting complex revealed by atomic force microscopy: functional significance for bacterial photosynthesis. *J Biol Chem* **279:** 21327–21333

Creighton TE (1993) *Proteins*. WH Freeman & Company: New York, NY

Deisenhofer J, Epp O, Miki K, Huber R, Michel H (1984) X-ray structure analysis of a membrane protein complex. *J Mol Biol* **180:** 385

Deisenhofer J, Epp O, Miki K, Huber R, Michel H (1985) Structure of the protein subunits in the photosynthetic reaction centre of *Rhodopseudomonas viridis* at 3 Å resolution. *Nature* **318:** 618–624

Deisenhofer J, Epp O, Sinning I, Michel H (1995) Crystallographic refinement at 2.3 Å resolution and refined model of the photosynthetic reaction centre from *Rhodopseudomonas viridis*. *J Mol Biol* **246:** 429–457

Deisenhofer J, Michel H (1989) NOBEL LECTURE: the photosynthetic reaction centre from the purple bacterium *Rhodopseudomonas viridis*. *EMBO J* **8:** 2149–2170

Engel A, Müller DJ (2000) Observing single biomolecules at work with the atomic force microscope. *Nat Struct Biol* **7:** 715–718

Francia F, Dezi M, Rebecchi A, Mallardi A, Palazzo G, Melandri BA, Venturoli G (2004) Light-harvesting complex 1 stabilizes P + QB-charge separation in reaction centers of *Rhodobacter sphaeroides*. *Biochemistry* (accepted)

Frese RN, Olsen JD, Branvall R, Westerhuis WH, Hunter CN, van Grondelle R (2000) The long-range supraorganization of the bacterial photosynthetic unit: a key role for PufX. *Proc Natl Acad Sci USA* **97:** 5197–5202

Germeroth L, Reiländer H, Michel H (1996) Molecular cloning, DNA sequence and transcriptional analysis of the *Rhodospirillum molischianum* B800/850 light-harvesting genes. *Biochim Biophys Acta* **1275:** 145–150

Gonçalves RP, Busselez J, Lévy D, Seguin J, Scheuring S (2004) Membrane insertion of *Rhodopseudomonas acidophila* light harvesting complex 2 (LH2) investigated by high resolution AFM. *J Struct Biol* (under revision)

Hartigan N, Tharia HA, Sweeney F, Lawless AM, Papiz MZ (2002) The 7.5-Å electron density and spectroscopic properties of a novel low-light B800 LH2 from *Rhodopseudomonas palustris*. *Biophys J* **82:** 963–977

Hu X, Damjanovic A, Ritz T, Schulten K (1998) Architecture and mechanism of the light-harvesting apparatus of purple bacteria. *Proc Natl Acad Sci USA* **95:** 5935–5941

Hu X, Ritz T, Damjanovic A, Autenrieth F, Schulten K (2002) Photosynthetic apparatus of purple bacteria. *Q Rev Biophys* **35:** 1–62

Jamieson SJ, Wang P, Qian P, Kirkland JY, Conroy MJ, Hunter CN, Bullough PA (2002) Projection structure of the photosynthetic reaction centre-antenna complex of *Rhodospirillum rubrum* at 8.5 Å resolution. *EMBO J* **21:** 3927–3935

Joliot P, Vermeglio A, Joliot A (1990) Electron transfer between primary and secondary donors in *Rhodospirillum rubrum*: evidence for a dimeric association of reaction centers. *Biochemistry* **29:** 4355–4361

Jungas C, Ranck J-L, Rigaud J-L, Joliot P, Vermeglio A (1999) Supramolecular organization of the photosynthetic apparatus of *Rhodobacter sphaeroides*. *EMBO J* **18:** 534–542

Koepke J, Hu X, Muenke C, Schulten K, Michel H (1996) The crystal structure of the light-harvesting complex II (B800–850) from *Rhodospirillum molischianum*. *Structure* **4:** 581–597

Kurisu G, Zhang H, Smith JL, Cramer WA (2003) Structure of the cytochrome b6f complex of oxygenic photosynthesis: tuning the cavity. *Science* **302:** 1009–1014

Marabini R, Masegosa IM, San Martin C, Marco S, Fernandez JJ, de la Fraga CG, Carazo JM (1996) Xmipp: an image processing package for electron microscopy. *J Struct Biol* **116:** 237–240

McDermott G, Prince SM, Freer AA, Hawthornthwaite-Lawless AM, Papiz MZ, Cogdell RJ, Isaacs NW (1995) Crystal structure of an integral membrane light-harvesting complex from photosynthetic bacteria. *Nature* **374:** 517–521

Montoya G, Cyrklaff M, Sinning I (1995) Two-dimensional crystallization and preliminary structure analysis of light harvesting II (B800–850) complex from the purple bacterium *Rhodovulum sulfidophilum*. *J Mol Biol* **250:** 1–10

Papiz MZ, Prince SM, Hawthornthwaite-Lawless AM, McDermott G, Freer AA, Isaacs NW, Cogdell RJ (1996) A model for the photosynthetic apparatus of purple bacteria. *Trends Plant Sci* **1:** 198–206

Papiz MZ, Prince SM, Howard TD, Cogdell RJ, Isaacs NW (2003) The structure and thermal motion of the B800–850 LH2 complex from *Rps. acidophila* at 2.0 Å resolution and 100 K: new structural features and functionally relevant motions. *J Mol Biol* **326:** 1523–1538

Ranck J, Ruiz T, Pehau-Arnaudet G, Arnoux B, Reiss-Husson F (2001) Two-dimensional structure of the native light-harvesting complex LH2 from *Rubrivivax gelatinosus* and of a truncated form. *Biochim Biophys Acta* **1506:** 67–78

Roszak AW, Howard TD, Southall J, Gardiner AT, Law CJ, Isaacs NW, Cogdell RJ (2003) Crystal structure of the RC–LH1 core complex from *Rhodopseudomonas palustris*. *Science* **302:** 1969–1972

Schabert FA, Engel A (1994) Reproducible acquisition of *Escherichia coli* porin surface topographs by atomic force microscopy. *Biophys J* **67:** 2394–2403

Schabert FA, Henn C, Engel A (1995) Native *Escherichia coli* OmpF porin surfaces probed by atomic force microscopy. *Science* **268:** 92–94

Scheuring S, Francia F, Busselez J, Melandri B, Rigaud J-L, Lévy D (2004a) Structural role of PufX in the dimerization of the photosynthetic core-complex of *Rhodobacter sphaeroides*. *J Biol Chem* **279:** 3620–3626

Scheuring S, Reiss-Husson F, Engel A, Rigaud J-L, Ranck J-L (2001) High resolution topographs of the *Rubrivivax gelatinosus* light-harvesting complex 2. *EMBO J* **20:** 3029–3035

Scheuring S, Seguin J, Marco S, Lévy D, Breyton C, Robert B, Rigaud J-L (2003a) AFM characterization of tilt and intrinsic flexibility of *Rhodobacter sphaeroides* light harvesting complex 2 (LH2). *J Mol Biol* **325:** 569–580

Scheuring S, Seguin J, Marco S, Lévy D, Robert B, Rigaud JL (2003b) Nanodissection and high-resolution imaging of the *Rhodopseudomonas viridis* photosynthetic core-complex in native membranes by AFM. *Proc Natl Acad Sci USA* **100:** 1690–1693

Scheuring S, Sturgis JN, Prima V, Bernadac A, Lévy D, Rigaud J-L (2004b) Watching the photosynthetic apparatus in native membranes. *Proc Natl Acad Sci USA* **101:** 11293–11297

Siebert CA, Qian P, Fotiadis D, Engel A, Hunter CN, Bullough PA (2004) Molecular architecture of photosynthetic membranes in *Rhodobacter sphaeroides*: the role of PufX. *EMBO J* **23:** 690–700

Stroebel D, Choquet Y, Popot JL, Picot D (2003) An atypical haem in the cytochrome b(6)f complex. *Nature* **426:** 413–418

Sturgis JN, Niederman RA (1990) Role of B800–850 light-harvesting pigment-protein complex in the morphogenesis of *Rhodobacter sphaeroides* membranes. In *Current Research in Photosynthesis*, Baltscheffsky M (ed) pp 57–60. Dordrecht: Kluwer

Sturgis JN, Niederman RA (1996) The effect of different levels of the B800–850 light-harvesting complex on intracytoplasmic membrane development in *Rhodobacter sphaeroides*. *Arch Microbiol* **165:** 235–242

Sundström V, Pullerits T, van Grondelle R (1999) Photosynthetic light-harvesting: reconciling dynamics and structure of purple bacterial LH2 reveals function of photosynthetic unit. *J Phys Chem B* **103:** 2327–2346

Tadros MH, Waterkamp K (1989) Multiple copies of the coding regions for the light-harvesting B800–850 alpha- and beta-polypeptides are present in the *Rhodopseudomonas palustris* genome. *EMBO J* **8:** 1303–1308

Unser M, Trus BL, Frank J, Steven AL (1989) The spectral signal-to-noise ration resolution criterion: computational efficiency and statistical precision. *Ultramicroscopy* **30:** 429–434

Unser M, Trus BL, Steven AC (1987) A new resolution criterion based on spectral signal-to-noise ratios. *Ultramicroscopy* **23:** 39–52

Walz T, Jamieson SJ, Bowers CM, Bullough PA, Hunter CN (1998) Projection structures of three photosynthetic complexes from *Rhodobacter sphaeroides*: LH2 at 6 Å, LH1 and RC-LH1 at 25 Å. *J Mol Biol* **282:** 833–845

Xia D, Yu CA, Kim H, Xia JZ, Kachurin AM, Zhang L, Yu L, Deisenhofer J (1997) Crystal structure of the cytochrome bc1 complex from bovine heart mitochondria. *Science* **277:** 60–66